JOURNAL OF Materials CHEMISTRY

Morphological properties of ultra-fine (Ni,Zn)-ferrites and their ability to decompose CO_2

Jung-Sik Kim,*[a] Jung-Ryul Ahn,[a] Chang Woo Lee,[b] Yasukazu Murakami[b] and Daisuke Shindo[b]

[a]*Department of Materials Science and Engineering, University of Seoul, Seoul 130-743, Korea. E-mail: jskim@uoscc.uos.ac.kr*
[b]*Institute of Multidisciplinary Research for Advanced Materials, Tohoku University, Sendai 980-8577, Japan*

Received 1st May 2001, Accepted 16th August 2001
First published as an Advance Article on the web 10th October 2001

Ultra-fine oxygen-deficient ferrites can decompose CO_2 gas, which causes the greenhouse effect, into C and O_2 at a low temperature of about 300 °C. In the present study, two ultra-fine powders of ternary ferrites of composition $(Ni,Zn)Fe_2O_4$, as potential catalysts for CO_2 decomposition, were prepared by hydrothermal synthesis or a coprecipitation method, and their abilities to decompose CO_2 investigated. X-Ray diffraction measurements identified the crystal structure of the ferrites as spinel-type. The Brunauer–Emmett–Teller (BET) surface area of the ferrite prepared by hydrothermal synthesis was above 110 $m^2\ g^{-1}$ and larger than for the sample obtained by the coprecipitation method. Particle sizes were very small, about 5–10 nm, in the both specimens. The CO_2 decomposition efficiency of the reduced oxygen-deficient ternary ferrite prepared by hydrothermal synthesis was better than that of the coprecipitation sample. The difference of the CO_2 decomposition efficiency is discussed in terms of the morphology and crystallinity based on TEM observations.

1. Introduction

The global warming of the earth, which is a serious environmental problem, is caused by emission of greenhouse gases such as carbon dioxide (CO_2), methane, nitrous oxide and perfluorocarbons. CO_2 is the major component of these emission gases. One possible approach to mitigate the emission of CO_2 would be to decompose it or to recycle it to give a useful product. Recently, it was shown that CO_2 could be actively decomposed to carbon and oxygen around 300 °C on the surface of oxygen-deficient ferrites $M_xFe_{3-x}O_{4-\delta}$ (M = divalent metallic ion), where δ is the oxygen deficiency.[1]

Until now, the reactivity of CO_2 decomposition in oxygen-deficient Zn(II)-, Mn(II)-, Co(II)- and Ni(II)-bearing ferrites has been widely studied, and it was claimed that the reactivity strongly depended on the processing methods and compositions. Particularly, the efficiency of CO_2 decomposition was improved significantly by developing particles of ultra-fine ferrites with a high specific surface area. Ferrites $M_xFe_{3-x}O_4$ themselves can be fabricated by a solid-state reaction. However, the conventional solid-state reaction at high temperature (above 1000 °C) produces large particle size crystalline ferrites, which results in a low CO_2 decomposition reactivity. In order to obtain ultra-fine ferrites and to investigate the CO_2 decomposition reactivity, many types of wet processing methods, such as the oxidation method,[2] coprecipitation,[3] and hydrothermal synthesis,[4] have been studied so far.

Most of the previous reports[5–7] mentioned that the particle composition, size, and BET surface area were responsible for the performance of CO_2 decomposition. Besides these factors, both the morphology and crystallinity of the particles will affect the performance, though this aspect requires further investigation. In the present study, we have synthesized ultra-fine powders of ternary (Ni,Zn)-ferrites by two distinct ways; hydrothermal synthesis and a coprecipitation method. Correlations of the morphology with the performance of CO_2 decomposition are discussed on the basis of transmission electron microscopy (TEM) observations for these specimens.

2. Experimental

Ultra-fine $(Ni_{0.5},Zn_{0.5})$-ferrites were synthesized by two distinct wet processings *i.e.* hydrothermal synthesis and a coprecipitation method. Measured stoichiometric amounts of $Ni(NO_3)_2\cdot 6H_2O$ (2.18 g), $Zn(NO_3)_2\cdot 6H_2O$ (2.23 g) and $Fe(NO_3)_2\cdot 6H_2O$ (12.12 g) were dissolved at 60 °C in distilled water (0.15 dm^{-3}) which was previously degassed with N_2 gas. The pH of solution was adjusted to a value of 9.0 by adding NaOH solution. The solution was held at 60 °C and stirred for the coprecipitation method. In the hydrothermal synthesis, the solution was neutralized with 3 mol dm^{-3} NaOH to a pH of about 9.0 as above and treated in an autoclave at 160 °C for 5 h. The precipitated products were separated by centrifuging at 10000 rpm, followed by washing with distilled water and ethanol, and then dried *in vacuo* at 60 °C for 20 h. Finally, the dried powders were heated at 300 °C in an N_2 atmosphere for 1 h to eliminate water and any hydroxy species.

The chemical compositions of synthesized ferrites were analyzed by inductively coupled plasma (ICP) spectroscopy. The crystalline phases were identified by X-ray diffractometry (XRD) with Cu-Kα radiation (Zeifert 3000). BET surface areas were determined by nitrogen adsorption (Shimadzu, Micromeritics 2400). The particles were dispersed in 1-butanol followed by agitation with an ultrasonic cleaner, and then placed on to microgrids covered with holey carbon films for TEM observations conducted using a JEM-2010 microscope operated at 200 kV or a JEM-3000F microscope at 300 kV.

CO_2 decomposition reactions were carried out in a continuous flow of 10% CO_2–90% N_2 which was controlled by a mass flow controller (MFC). About 1.0 g of reduced (Ni,Zn)-ferrite powder was placed in a quartz tube of 10 mm inner

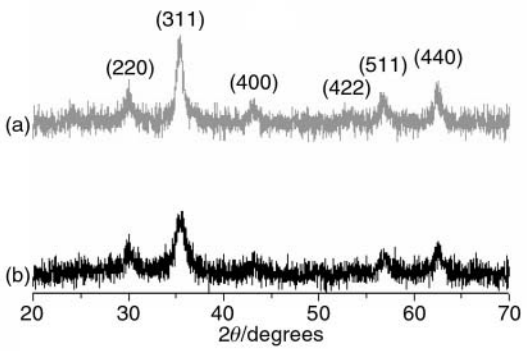

Fig. 1 X-Ray diffration patterns of $(Ni_{0.5},Zn_{0.5})Fe_2O_4$ ferrites synthesized (a) hydrothermally and (b) by coprecipitation.

Table 1 Chemical composition, BET surface area, lattice parameter and average particle size of $Ni_{0.5}Zn_{0.5}Fe_2O_4$ ferrites

Sample process	Composition	Lattice parameter/nm	Particle size/nm	BET surface area/$m^2\ g^{-1}$
Hydrothermal synthesis	$Ni_{0.49}Zn_{0.51}$-$Fe_{2.00}O_4$	0.8410	8.5	113.2
Coprecipitation method	$Ni_{0.51}Zn_{0.50}$-$Fe_{1.99}O_4$	0.8407	7.0	77.6

diameter heated by a tubular electric furnace. The efficiency of CO_2 decomposition was analyzed by using gas chromatography (Shimadzu, GC-8A instrument equipped with a thermal conductivity detector).

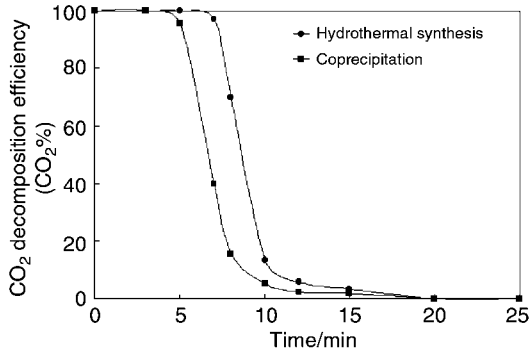

Fig. 2 Comparison of CO_2 decomposition efficiency for $(Ni_{0.5},Zn_{0.5})$-$Fe_2O_{4-\delta}$ synthesized by hydrothermal synthesis and the coprecipitation method. The efficiency corresponds to the fraction of decomposed CO_2 with respect to the initial CO_2 in the flowing gas of 10% CO_2–90% N_2.

3. Results and discussions

Fig. 1 shows the XRD spectra of $(Ni_{0.5}Zn_{0.5})Fe_2O_4$, prepared by hydrothermal synthesis (a) and coprecipitation (b), respectively, where the chemical formula assumes the molar ratio of Fe and oxygen to be stoichiometric. The XRD patterns verified that the specimens are single phases with spinel-type structure. The observable peaks are broad since the size of particles is small. The average particle sizes calculated with the Scherrer equation,[8] where the peak of 311 was analyzed, were 8.5 nm for the hydrothermal sample and 7.0 nm for the coprecipitation sample, while the corresponding BET surface areas were 113.2 and 77.6 $m^2\ g^{-1}$. Table 1 summarizes the

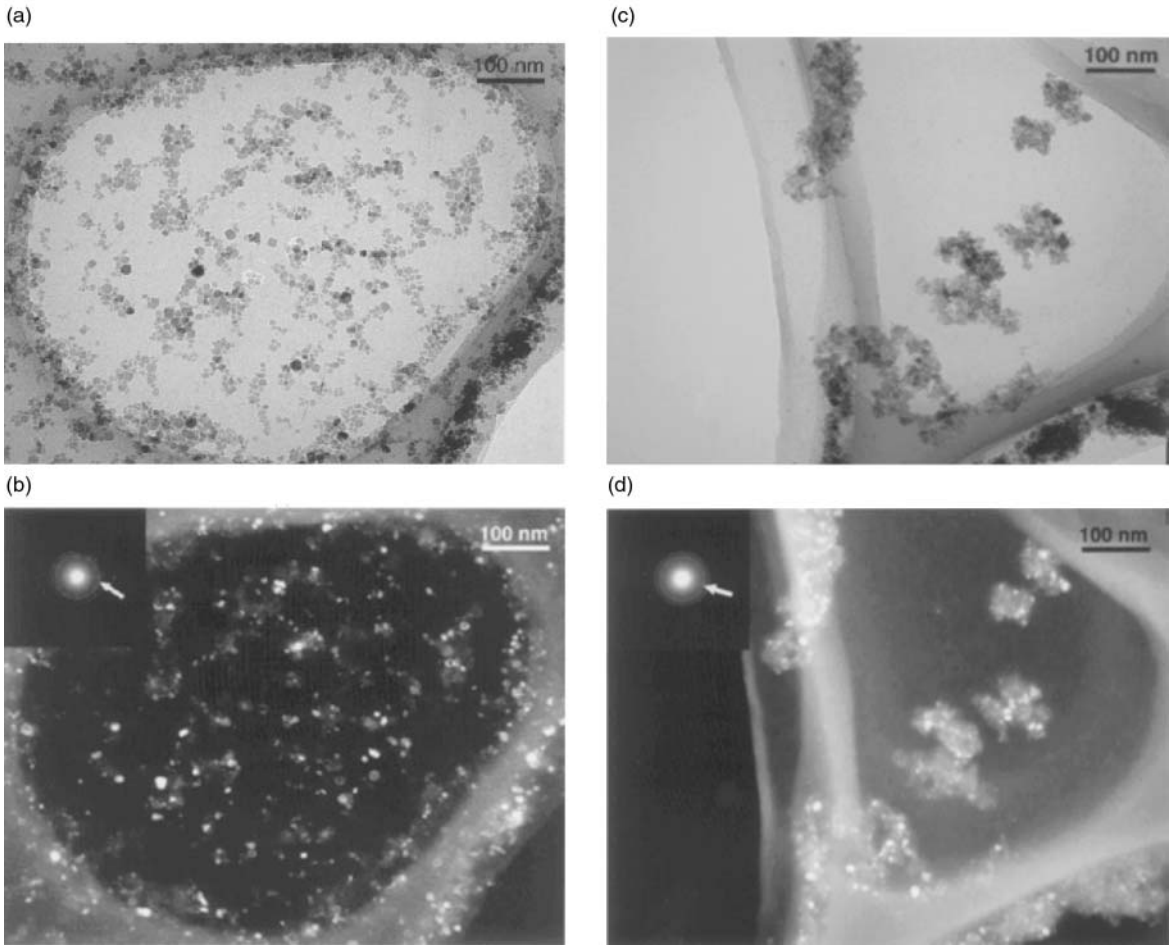

Fig. 3 A set of bright and dark field images for $(Ni_{0.5},Zn_{0.5})Fe_2O_4$ powders obtained by hydrothermal synthesis (a and b), and by the coprecipitation method (c and d), respectively. The dark field image was obtained with the [311] reflection marked as an arrow in the inset.

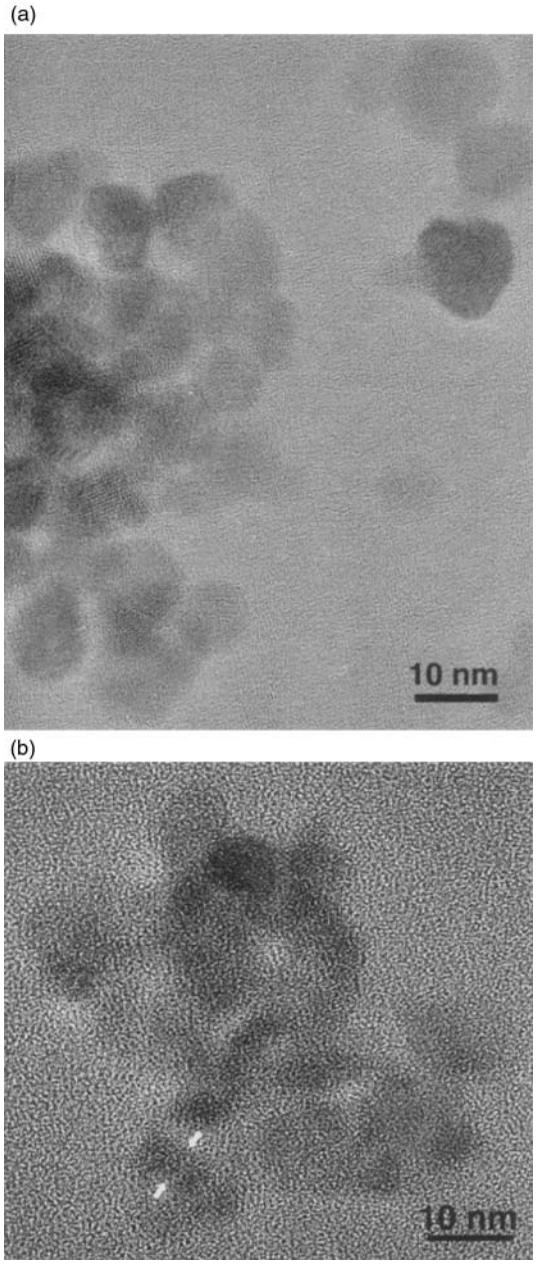

Fig. 4 Lattice images for $(Ni_{0.5},Zn_{0.5})Fe_2O_4$ ferrites obtained by hydrothermal synthesis (a) and the coprecipitation method (b).

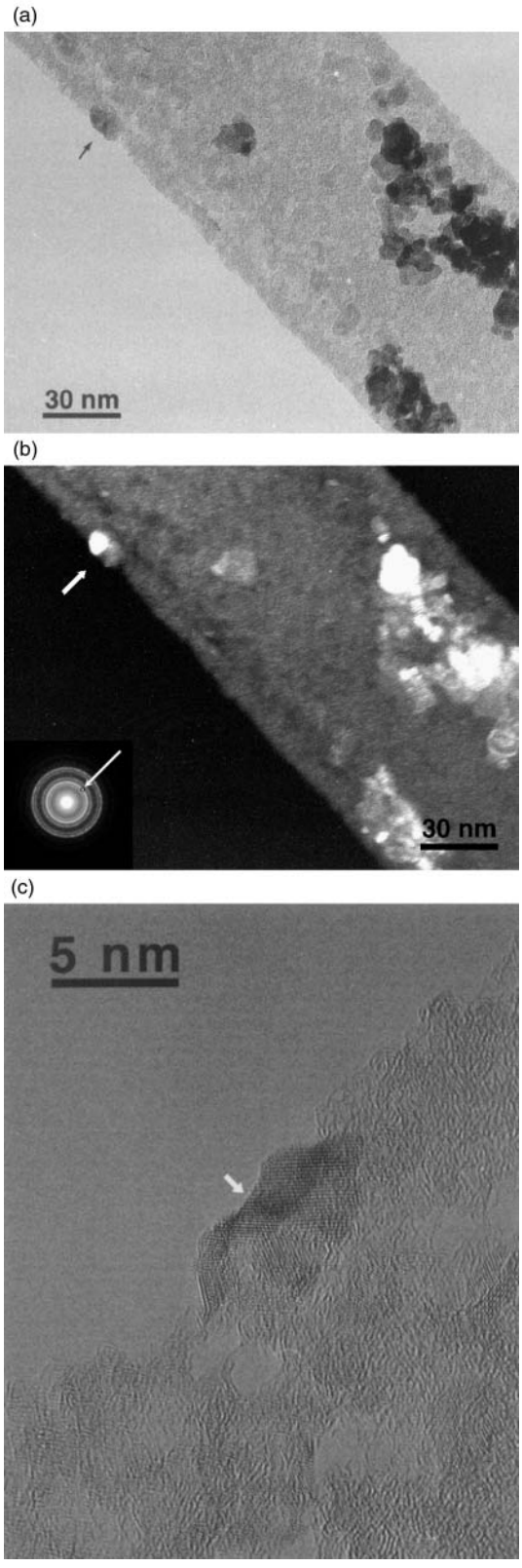

Fig. 5 A set of (a) bright and (b) dark field images and (c) lattice images for $(Ni_{0.5},Zn_{0.5})Fe_2O_4$ ferrites obtained by coprecipitation. The dark field image was obtained with the [311] reflection marked as an arrow in the inset.

results of the chemical composition, BET surface area, lattice parameter and particle size obtained by XRD for the two samples. The lattice parameters were calculated from the XRD peaks at 220, 311, 400, 422, 511 and 440, with the aid of extrapolation by the Nelson–Riley function.[8] The chemical compositions of the $(Ni_{0.5},Zn_{0.5})$-ferrites were nearly the stoichiometric compositions: $(Ni_{0.49}Zn_{0.51})Fe_{2.00}O_4$ for the hydrothermal synthesis sample and $(Ni_{0.51}Zn_{0.50})Fe_{1.99}O_4$ for the coprecipitation sample. The (Ni,Zn)/Fe mole ratio of the (Ni,Zn)-ferrites was nearly the same as that of the starting solution for the preparation (0.5).

Fig. 2 compares the performance of CO_2 decomposition for the reduced $Ni_{0.5}Zn_{0.5}Fe_2O_{4-\delta}$ ferrites synthesized by the two different methods, *i.e.* the coprecipitation method and hydrothermal synthesis. These oxygen-deficient ferrites, $Ni_{0.5}Zn_{0.5}$-$Fe_2O_{4-\delta}$, were formed by hydrogen reduction at 300 °C for 3 h. Then feed gas of 10% CO_2–90% N_2 was passed at a flow rate of 60 ml min^{-1} through the reaction cell held at 300 °C in which 1 g of the reduced ferrite was placed. As clearly seen in Fig. 2, the ferrite obtained *via* hydrothermal synthesis continued to decompose CO_2 completely for 7 min and showed a better efficiency for CO_2 decomposition than the coprecipitation sample.

In order to examine the relation of the morphology with the CO_2 decomposition performance, TEM observations were carried out for the ferrites synthesized by the two distinct processing methods. Fig. 3(a) and (b) show bright and dark

field images of particles synthesized by the hydrothermal method, respectively, while Fig. 3(c) and (d) show those of the coprecipitation sample. The particles synthesized by the hydrothermal synthesis are spherical and dispersed uniformly, whereas those obtained by coprecipitation are irregularly shaped and clustered. This indicates that particles obtained by hydrothermal synthesis have better crystallinity than those *via* the coprecipitation method. Also, the selected area electron diffraction (SAED) pattern (left top of dark field images in Fig. 3) of particles by the hydrothermal synthesis show sharper rings or spots than those *via* the coprecipitation method. This result is also consistent with that from the XRD spectra in Fig. 1.

Fig. 4 compares lattice images of the two specimens, prepared by hydrothermal synthesis (a) and the coprecipitation method (b). The lattice fringe of the hydrothermal particles is much clearer compared with that of the coprecipitation particles. Even when the morphology is observed at a high magnification, the hydrothermal particles seem spherical, well dispersed and without considerable clustering, and the particle size is almost uniform, *i.e.* about 9 nm in diameter. This average particle size agrees well with that calculated from XRD spectra (Table 1, $\sim$8.5 nm). On the other hand, the coprecipitation particles are irregularly shaped, ranging from 5 to 7 nm in diameter, and clustered or coalesced with each other. For example, a cluster marked by the arrows in Fig. 4(b) consists of two distinct particles. In order to obtain a clearer evidence of the coalescence of particles for the coprecipitation sample, dark field images were analyzed in detail. Fig. 5 shows a set of bright field (a) and dark field (b) images of the same area for coprecipitation particles. Here, Fig. 5(b) was obtained with the [311] reflection marked by an arrowhead in the inset. Although the cluster indicated by an arrow in Fig. 5(a) seems to be a single crystal particle, only the left half is bright in the dark-field image of Fig. 5(b), indicating that the particle is polycrystalline. Also, Fig. 5(c), the lattice image for this particle, clearly shows the presence of some grain boundaries within the particle.

The average size of particles synthesized by the coprecipitation method is larger than those obtained *via* hydrothermal synthesis, and hence the BET surface area of the former sample is less than that of the latter. However, the present TEM observations showed that the difference of particle size was fairly small between the two samples. By contrast, the morphology and shape were quite different for the two samples. Particles by the coprecipitation method are irregularly shaped, coalesced and clustered to each other, while those *via* hydrothermal synthesis are spherical, homogeneous and dispersed without appreciable clustering. Also, the crystallinity of particles prepared by the hydrothermal synthesis was superior to that by the coprecipitation method. We believe that this clustering or coalescence is responsible for the lower efficiency of CO_2 decomposition for particles prepared by the coprecipitation method.

4. Conclusions

Ultra-fine (Ni,Zn)-ferrites with particle size less than 10 nm were synthesized by a coprecipitation method and by hydrothermal synthesis. Oxygen-deficient (Ni,Zn)-ferrite synthesized by the hydrothermal synthesis showed better CO_2 decomposition efficiency than that obtained *via* the coprecipitation method. TEM observations revealed that the particles obtained by hydrothermal synthesis showed a homogeneous spherical shape, and they were well dispersed without an appreciable clustering. By contrast, the particles obtained by the coprecipitation method were irregular in shape, and coalesced and clustered with each other. It is concluded that ferrite particles with good crystallinity, spherical shape, and dispersed distribution have a high CO_2 decomposition reactivity.

Acknowledgements

This work was partially supported by the Korean Energy Management Corporation. The authors thank the Japan Society for the Promotion of Science (JSPS) and the Korea Science and Engineering Foundation (KOSEF) for enabling one of the authors to visit Tohoku University for a month through their financial support.

References

1 Y. Tamaura and M. Tabara, *Nature (London)*, 1990, **346**, 255.
2 M. Tsuji, T. Kodama, T. Yoshida, Y. Kitayama and Y. Tamaura, *J. Catal.*, 1996, **164**, 315.
3 M. Tsuji, Y. Wada, T. Yamamoto and T. Tamaura, *J. Mater. Sci. Lett.*, 1996, **15**, 156.
4 S. Komarneni, M. Tsuji, Y. Wada and Y. Tamaura, *J. Mater. Chem.*, 1997, **7**, 2339.
5 T. Yoshida, M. Tsuji, Y. Tamaura, T. Hurue, T. Hayashida and K. Ogawa, *Energy Convers. Mgmt.*, 1997, **38**, Suppl., S443.
6 T. Kodama, H. Kato, S. G. Chang, N. Hasegawa, M. Tsuji and Y. Tamaura, *J. Mater. Res.*, 1994, **9**, 462.
7 H. Kato, T. Kodama, M. Tsuji and Y. Tamaura, *J. Mater. Sci.*, 1994, **29**, 5689.
8 B. D. Cullity, *Elements of X-ray diffraction*, Addison-Wesley Pub. Co., MA, 2nd edn., 1978, pp. 101, 356.